

NUMERICAL SIMULATION OF A BUOYANT SUSPENDING DROP IN PLANE COUETTE FLOW: THE EQUILIBRIUM POSITION OF THE DROP*

S. GOODARZI** AND S. MORTAZAVI

Dept. of Mechanical Engineering, Isfahan University of Technology, Isfahan 84156-83111, I. R. of Iran
Email: s.goodarzi@me.iut.ac.ir

Abstract– The lateral migration of a two-dimensional buoyant drop in simple shear flow is studied numerically. For a slightly buoyant drop, the drop migrates to an equilibrium position which is close to the walls depending on whether the drop leads or lags the flow. If the drop is relatively more buoyant, the equilibrium position moves back to the midplane. The equilibrium position of the drop depends on the Froude number of the flow. The behavior has been investigated for various Froude numbers. The equilibrium position also depends on the drop deformation. When the Capillary number is raised, the equilibrium position moves away from the wall. At relatively large Capillary numbers, the drop shape is not stable, and the equilibrium position shows small oscillations due to an unstable drop shape. The effect of the Reynolds number on the equilibrium position has also been studied by a few simulations. It is found that at a relatively large Reynolds numbers ($Re_h = 80$) and a moderate Froude number ($Fr = 160$) the drop oscillates with a finite amplitude inside the channel. The equilibrium position of the drop agrees qualitatively with perturbation theories and numerical results available for solid particles.

Keywords– Non-neutrally buoyant drop, shear flow, density ratio, capillary number, froude number, Reynolds number

1. INTRODUCTION

Many fluids contain buoyant particles that are either rigid or deformable. Polymeric liquids, fuel sprays, and red blood cells are just a few examples. A common phenomenon with such fluid systems is the concentration gradient of particles across the channel, which is of great importance in polymer processing. Taylor [1] appears to be the first to have experimentally studied this phenomenon. In fuel sprays, if the drop size is relatively small, the effect of gravity on the motion of drop is negligible. The wall repulsion of drops was also observed by Karnis and Mason [2] experimentally. They observed that liquid drops migrate away from the walls in plane Couette flow at small Reynolds numbers, and reached equilibrium about half way between the two walls. Experiments performed by Halow and Wills [3] at non-zero Reynolds numbers with solid particles, showed that particles also migrate away from the walls in circular Couette flow. But the particles did not settle exactly to the midplane of the gap. They further suggested that the off-center deviation was due to experimental error or the curvature of the velocity profile. As far as we know, the work by Vasseur and Cox [4] is the only theoretical and experimental study that addresses the migration of buoyant particles. In the limit of small particles and vanishing Reynolds numbers, their perturbation analysis showed that in a plane Couette flow, if the particle leads the fluid (a lighter particle in upward flow or a heavier particle in downward flow), it migrates to the stationary wall. A lagging particle, however, migrates to the moving wall. Perturbation theories of viscous or inertial type are valid

*Received by the editors October 27, 2011; Accepted March 11, 2012.

**Corresponding author

for small particle Reynolds numbers, i.e. $Re_p \ll \xi^2$ (Ho and Leal [5]), where ξ is the ratio of particle radius to channel height. This restriction is relaxed in our study.

The migration of deformable drops in a shear flow has been studied by numerical simulations using boundary-integral method at zero Reynolds number. Zhou and Pozrikidis [6, 7] performed a two-dimensional simulation of a single drop and a few droplets in a plane Couette flow at zero Reynolds number. They showed that deformable drops migrate away from the walls, and the suspension exhibits a shear-thinning behavior. Feng et al [8] reported the results of a two-dimensional finite element simulation of the motion of a circular particle in a plane Couette flow. They discovered that several mechanisms are responsible for the lateral migration of rigid particles in shear flows: a) drift by the walls that mainly forces particles away from the walls, b) migration of particles due to the effect of inertia, provided that a slip velocity exists between the particle and the local undisturbed flow (the slip velocity is defined as the particle velocity minus the local undisturbed velocity at the center of the particle), c) migration due to the rotation of particle along with a slip velocity which is known as Magnus lift. Saffman [9] found that, under creeping conditions, the inertial lift exerted on a spherical particle in an unbounded shear flow follows the relationship:

$$\Lambda = 6.46\rho Ua^2(\nu G)^{1/2} = 6.46\rho\nu Ua Re^{1/2} \quad (1)$$

where ν is the kinematic viscosity, U is the slip velocity of the particle and $Re = Ga^2/\nu$ is the Reynolds number defined based on the shear rate (G) and particle radius (a).

Kapil and Pozrikidis [10] considered simple shear flow of a one-dimensional array of two-dimensional viscous drops with constant surface tension at small and moderate Reynolds numbers. Their results established a critical Capillary number that specifies the onset of drop breakup. When the physical properties of the drop are fixed, inertial effects tend to promote drop deformation.

Mortazavi and Tryggvason [11] studied the motion of a single drop at non-zero Reynolds numbers in Poiseuille flow. The migration of the drop was studied as a function of the Reynolds number, the Weber number and the viscosity ratio. Matas et al. [12] investigated mechanisms of lateral migration for neutrally and non-neutrally buoyant rigid particle in simple shear flow.

Liu and Lu [13] studied the migration of deformable drops in channel flow neglecting the gravity influence at finite Reynolds numbers. They discussed the effects of some typical parameters such as, the Reynolds number, the Weber number, the viscosity ratio and the density ratio.

Lin and Guo [14] made an experimental study about the deformation and breakup of a single drop immersed in a Newtonian liquid. They investigated the dynamic transitions of nonstationary deformation and breakup of drops characterized by large capillary numbers.

Recently, Bayareh and Mortazavi [15] investigated three-dimensional numerical simulation of a drop in simple shear flow at finite Reynolds numbers. They found that the midplane of the channel is a stable equilibrium position for the drop. Also, Mortazavi et al. [16] studied the motion of deformable drops suspended in a simple shear flow at a wide range of Reynolds numbers. They found that at a relatively large Reynolds number, the drop migrates to an equilibrium position which is a little off the mid-plane.

In the present work, the motion of a two-dimensional, neutrally and non-neutrally buoyant drop is studied in a simple shear flow by numerical simulations at finite-Reynolds-numbers. The effect of Froude number, density ratio, Reynolds number and Capillary number is investigated.

2. GOVERNING EQUATIONS AND DIMENSIONLESS PARAMETERS

The equations governing unsteady motion of viscous, incompressible, immiscible two-fluid systems are the Navier-Stokes equations; in conservative form we have:

$$\frac{\partial \rho \mathbf{u}}{\partial t} + \nabla \cdot (\rho \mathbf{u} \mathbf{u}) = -\nabla p + \nabla \cdot \mu (\nabla \mathbf{u} + \nabla \mathbf{u}^T) - \int (\sigma \kappa \mathbf{n}) \delta^\beta (\mathbf{x} - \mathbf{X}(s, t)) ds + \rho \mathbf{F} \quad (2)$$

where \mathbf{u} is the fluid velocity, ρ is the density, p is the pressure, μ is the viscosity, and σ is the surface tension coefficient. Also, δ is a two- or three-dimensional delta function corresponding to $\beta = 2$ and $\beta = 3$, respectively, κ is the curvature for two-dimensional flows and twice the mean curvature for three-dimensional flows, \mathbf{n} is a unit vector normal to the drop surface pointing outside of the drop, \mathbf{x} is the position in the Eulerian coordinate, \mathbf{X} is the position of the front in Lagrangian coordinate, \mathbf{F} is a body force which is the gravity force (g) in the current problem.

Both fluids are taken to be incompressible, so the divergence of velocity field is zero:

$$\nabla \cdot \mathbf{u} = 0 \quad (3)$$

Equations of state for the density and the viscosity are:

$$\frac{D\rho}{Dt} = 0 \quad (4)$$

$$\frac{D\mu}{Dt} = 0 \quad (5)$$

These equations show that the density and the viscosity of a fluid element remain constant. The geometry of the flow is shown in Fig. 1. It comprises two parallel plates of infinite width with one of them fixed and the other one moving at a constant speed, U . A drop of radius a with density ρ_i and viscosity μ_i is seen to be suspending in a Newtonian fluid with density ρ_o and viscosity μ_o . The computational domain is periodic in the x -direction and bounded by the no-slip walls in the y -direction.

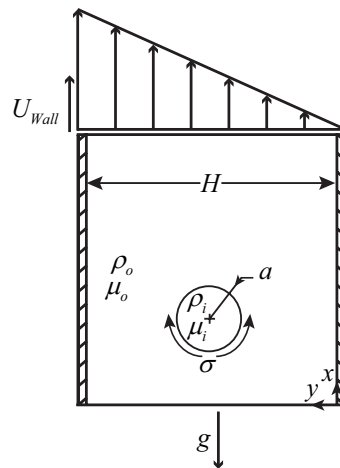


Fig. 1. Schematic showing the flow geometry

The pertinent dimensionless numbers are: i) the ratio of the viscosity of the drop fluid to the suspending medium $\lambda = \mu_i / \mu_o$, ii) the density ratio $\alpha = \rho_i / \rho_o$ (the viscosity and density of the drop liquid are denoted by μ_i and ρ_i , and those due to the surrounding fluid are μ_o, ρ_o), iii) the ratio of the drop radius to the height of the channel $\xi = a / H$ (ξ is taken as 0.125 in our study), iv) the Reynolds number, v) the Froude number, and vi) the Capillary number. The Reynolds number is defined in different ways: A bulk Reynolds number is defined based on the shear rate and channel height ($Re_b = \rho_o G H^2 / \mu_o$), and a particle Reynolds number is defined based on the shear rate and drop radius ($Re_p = \rho_o G a^2 / \mu_o$), where a is the drop radius. For computations in this paper, we use a bulk Reynolds number from 5 to 80. So, the particle Reynolds number changes from 0.078 to 1.25. The shear rate is $G = U_{wall} / H$ where U_{wall}

is the velocity of the top wall, (the bottom wall is fixed). The Capillary number ($Ca = Ga\mu/\sigma$) describes the ratio of the viscous stress to the interfacial tension. The Froude number is defined as: $Fr = gH/U_{wall}^2$. Dimensionless time is defined by: $\tau = tG$. In the current work, the ratio of the viscosity of drop fluid to that of the ambient fluid is assumed to be equal to one.

The effective viscosity of a suspension under a uniform shear rate can be obtained from:

$$\mu_{eff} = \frac{\langle \sigma_{12} \rangle}{G} = \frac{2\mu_o \langle e_{12} \rangle + \frac{1}{A} \int_{S_D} \sigma \kappa n_1 x_2 dl - \frac{\rho}{A} \int_A u'_1 u'_2 dA}{G} \quad (6)$$

where u' is the fluctuation velocity, S_D is the total surface of drop, dl is an elemental line segment of the interface. The derivation of the above formula can be found in reference [7].

3. NUMERICAL METHOD

Various methods have been used to simulate two-phase flows. These methods include the Marker-And-Cell (MAC), the Volume-Of-Fluid (VOF), and the level set method. In general, the interface representation can be explicit (moving mesh) or implicit (fixed mesh) or a combination of both. The front-tracking method is a combination of fixed and moving mesh method. Although an interface grid tracks the interface, the flow is solved on a fixed grid. The interface conditions are satisfied by smoothing the interface discontinuities and interpolating interface forces from the interface grid to the fixed grid. The governing equations for the flow of drops in a channel are solved by a Finite Difference/Front Tracking method developed by Unverdi and Tryggvason [17, 18]. A second order projection method is used to solve the Navier-Stokes equations on a staggered grid. Both the convective and diffusion terms are discretized by central differencing and a second order predictor-corrector scheme is used for time marching. The interface between the two fluids is represented by marker points that are advected by the flow velocity. The surface tension is calculated by finding the curvature of this moving grid, and distributing it onto the stationary grid. When the density ratio is one, the elliptic equation for pressure is solved by a fast Poisson solver (FISH PACK), but when the density of the drop is different from that of the suspending fluid, the equation for the pressure field is solved by a Multigrid method (Adams [19]).

4. RESULTS

a) Grid independency

To investigate the dependence of the results to grid resolution, resolution tests have been performed at different Reynolds numbers, Froude numbers and density ratios. Figure 2(a) shows the lateral position versus the axial location for a drop at $Re_b = 10$, $Fr = 392$, $\rho_i/\rho_o = 1.002$ and $Ca = 0.0048$ for three different computational grids. The Froude number is the same as that examined by Feng et al. [8] for solid particles. Since the density ratio is greater than one drop, the drop obtains a negative slip velocity. Thus the Magnus type lift force points towards the upper wall, and the drop reaches an equilibrium position in the upper half plane. The equilibrium position is a result of the balance between the force due to the presence of the walls (lubrication effect) and the aforementioned Magnus type lift. It is observed that the lateral equilibrium position changes slightly as the grid is refined. The equilibrium positions are relatively close at high grid resolutions (128×128 and 192×192 grids).

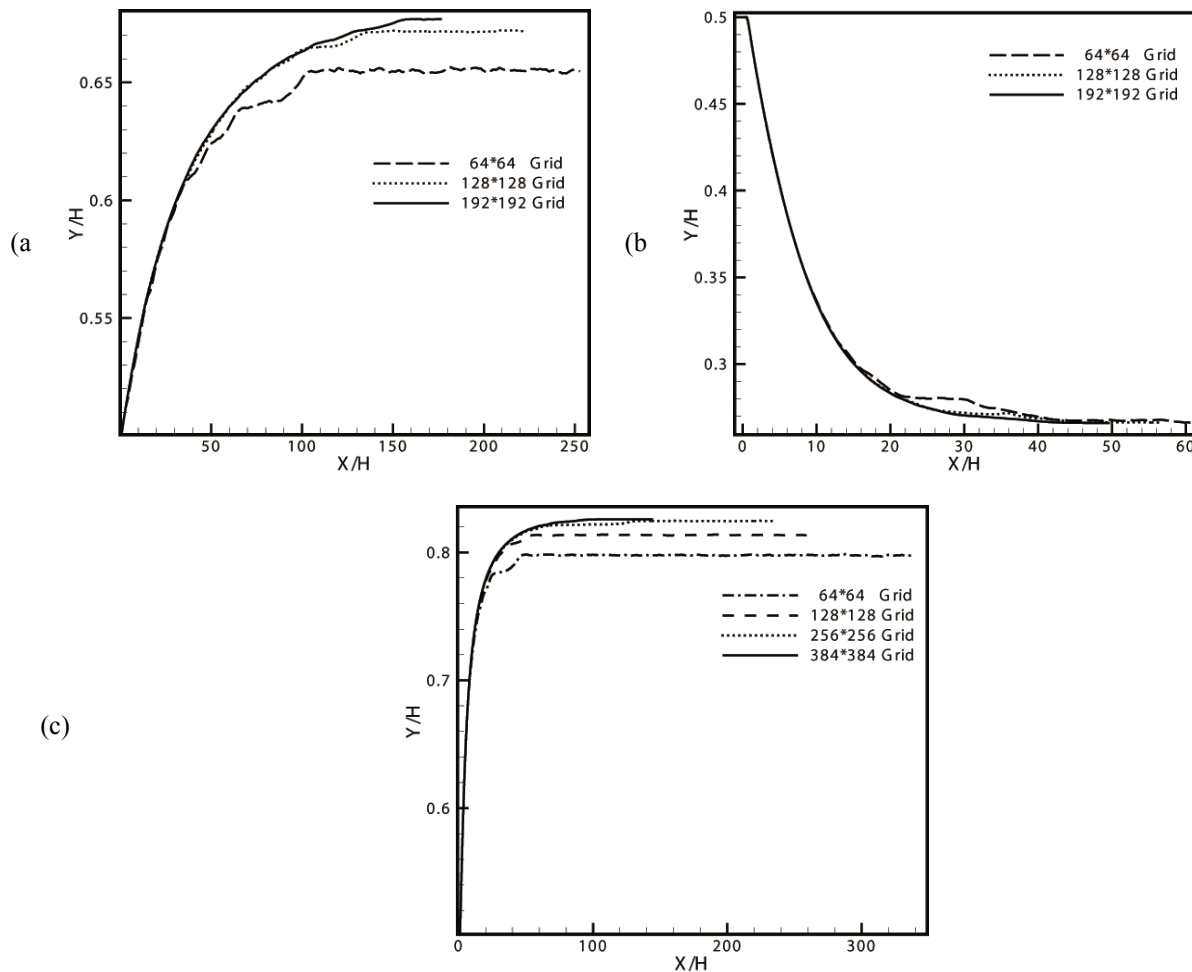


Fig. 2. Effect of resolution on the lateral migration of a drop in a simple shear flow, (a) $Re_b = 10$, $Fr = 392$, $\rho_i/\rho_o = 1.002$, $Ca = 0.0048$, (b) $Re_b = 10$, $Fr = 160$, $\rho_i/\rho_o = 0.95$, $Ca = 0.0048$, (c) $Re_b = 40$, $Fr = 10$, $\rho_i/\rho_o = 1.05$, $Ca = 0.0048$

Figure 2b presents similar results for a drop at $Re_b = 10$, $Fr = 160$, $\rho_i/\rho_o = 0.95$ and $Ca = 0.0048$. Here, since the density ratio is smaller than unity, the drop leads the undisturbed flow (the slip velocity is positive). As a result, the Magnus type lift is towards the bottom wall, and the drop migrates to an equilibrium position in the lower half plane. The figure also shows very little change in the equilibrium position as the grid is refined. This is due to the lower Froude number chosen in this case. In other words, if the drop is less buoyant (lower Froude number), lower grid resolution is needed to resolve the flow. A grid study has also been undertaken at a higher Reynolds number, namely $Re_b = 40$.

Figure 2c depicts results at four grid resolutions for this case. Again, higher grid resolution is required as the Reynolds number is raised. It is clearly seen that the equilibrium position of the drops is close at high grid resolutions (256×256 and 384×384 grids). But the result is a little different from the forgoing cases at a low grid resolution (64×64 grids).

The present results agree with the numerical simulation of Feng et al. [8] for solid particles and perturbation theory of Vasseur and Cox [4]. The differences for the equilibrium position are due to deformation of drops and the internal circulation inside the drop.

b) Effect of density ratio

Numerical simulations were carried out at different density ratios using a Reynolds number of $Re_b = 40$, a Froude number of $Fr = 10$, and a Capillary number of $Ca = 0.0048$. The grid resolution

for all cases is 256×256 grid points. The case is similar to that considered by Feng et al. [8], except that the Froude number is smaller ($Fr = 392$ in Feng et al. [8] simulations). We note that a larger range of density ratios was used here compared to that examined by Feng et al. [8]. So, the Froude number was reduced in order to consider a broad range of density ratios. If the Froude number is sufficiently large, then a stable equilibrium position may not be obtained for density ratios that deviate considerably from one. Figure 3(a) shows the lateral position of a drop versus the axial location at different density ratios. Results are in qualitative agreement with those found by Feng et al. [8]. When the density ratio is close to one (0.998, 0.95, 1.002, 1.01 and 1.05), the equilibrium position of the drop moves to one of the walls depending on whether the drop is lighter or heavier than the surrounding fluid. In other words, for slightly buoyant drops, the drop migrates to an equilibrium off the center line. The equilibrium position gets closer to the walls as the density ratio is raised or reduced (larger or smaller than one). We recall that there are three mechanisms responsible for lateral migration of a particle in a shear flow: the inertial lift, the lubrication effect due to the presence of the walls, and a rotational lift (Magnus effect). For a light drop, the drop leads the flow, so the rotational lift and inertial lift are towards the stationary wall. Therefore, the drop obtains a stable equilibrium position in the lower half plane where the wall repulsion balances the forgoing forces. For a heavier drop, however, the slip velocity is negative (the drop lags the flow), so the inertial lift and rotational lift point towards the moving wall. As a result, the equilibrium position of the drop moves to the upper half plane. When the density ratio is increased or reduced further, the magnitude of the slip velocity gets larger (Fig. 3b). This moves the equilibrium position of the drop closer to the walls. This trend reverses at large or small density ratios (0.8, 1.2). The same behavior has been observed by Feng et al. [8]. For moderately buoyant drops the equilibrium position of the drop moves back to the center line. In these density ratios the magnitude of the slip velocity is considerably large (Fig. 3b). The lift due to inertia or Saffman lift force [9] decreases at large slip velocities. This has been shown by McLaughlin [20].

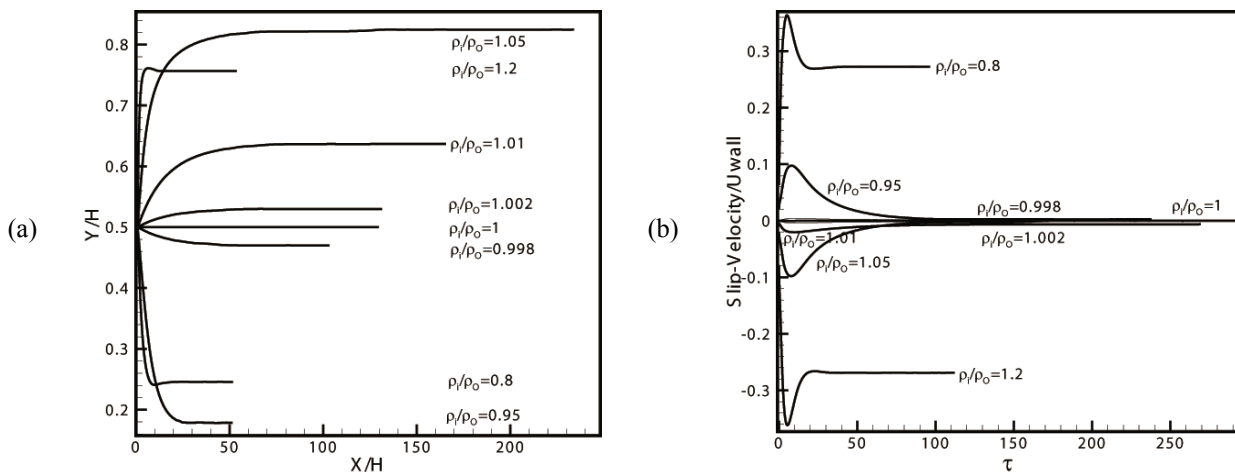


Fig. 3. (a) The lateral position of drop versus the axial location for $Re_b = 40$, $Fr = 10$ and $Ca = 0.0048$, (b) the slip velocity of drop versus time

The rotation of the drop also decreases at large slip velocities. The circulation around the drop (not plotted here) decreases when the density ratio deviates significantly from one. This is reasonable since the effect of the velocity gradient due to the shear flow across the drop is suppressed when the slip velocity is large. Therefore the lift due to the rotation of the drop is reduced. However, the wall repulsion (lubrication effect) is greatly amplified at large slip velocities. The increased wall repulsion forces the drop away from the wall. As a result, the equilibrium position of the drop moves away from the walls (towards the midplane) at large or small density ratios.

The streamlines relative to an observer moving with the drop are plotted in Fig. 4 at two density ratios. The streamlines are at a state where the drop has obtained a stable equilibrium position. When the density ratio is close to one (1.05), the slip velocity is small, and the effect of the external shear field is dominant. So, the streamlines show a unique circulation zone inside the drop (Fig. 4a). At a low enough density ratio (0.8), the slip velocity is large, so the flow is dominated by slip velocity. The drop behaves like a rising bubble relative to the external flow field, and two circulation zones appear inside the drop (Fig. 4b).

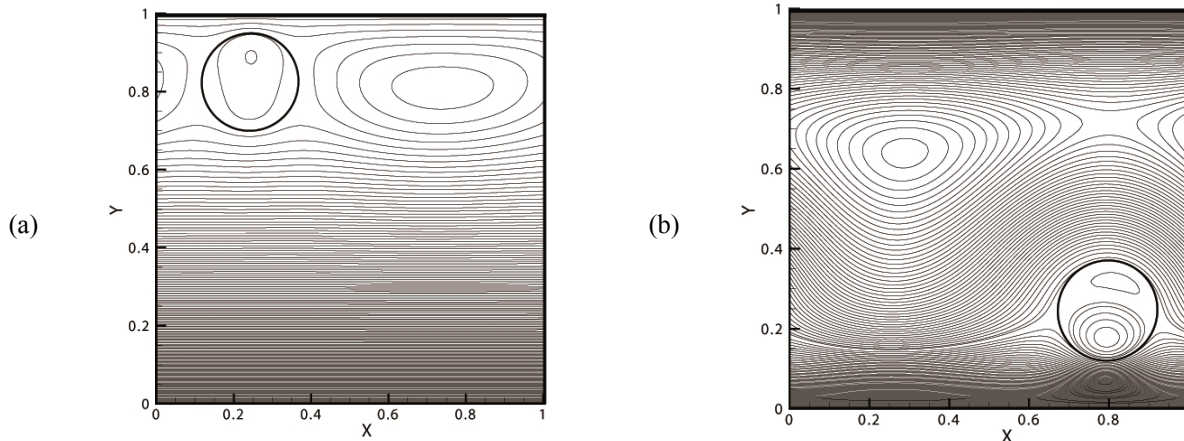


Fig. 4. Streamlines for drops at stable equilibrium position, $Re_b = 40$, $Fr = 10$ and $Ca = 0.0048$, (a) $\rho_i/\rho_o = 1.05$, (b) $\rho_i/\rho_o = 0.8$

The equilibrium position of the drop is plotted against the density ratio for two Froude numbers in Fig. 5. The variation of the equilibrium position with density ratio is stronger at higher Froude number. A large Froude number imposes a large buoyancy force in the flow, and consequently the equilibrium position shows fast variations with density ratio. The figure also shows a maximum and minimum equilibrium position which occurs at two specific density ratios.

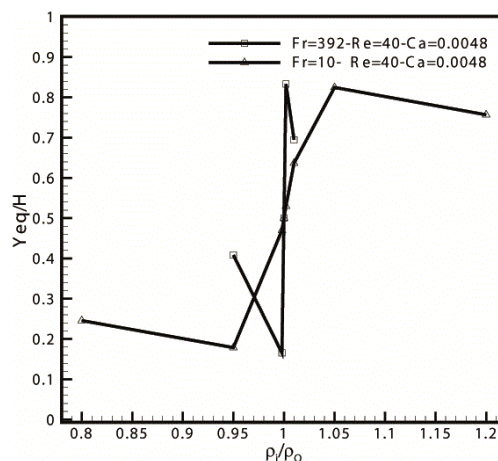


Fig. 5. Equilibrium position versus density ratio for two Froude numbers, $Re_b = 40$ and $Ca = 0.0048$

c) Effect of deformation

The effect of deformation on the lateral equilibrium position of the drop was investigated using different Capillary numbers. Figure 6a presents the lateral position versus the axial location of a drop at $Re_b = 40$, $Fr = 10$ and $\rho_i/\rho_o = 1.05$. A broad range of Capillary numbers was considered (0.0048 to 0.48). As the Capillary number is reduced, the equilibrium position moves towards the upper wall. The

drop shapes at steady state equilibrium positions are shown in Fig. 6b. As expected, the drop deformation increases with increasing the Capillary number. This enhances the wall repulsion force. A deformable particle receives a larger force than a circular one due to the presence of the wall. This has been observed by Zhou and Pozrikidis [6, 7] and Mortazavi and Tryggvason [11] in their numerical simulation of drops suspended in shear flows. Also, since the density ratio is greater than one, the rotational lift is towards the moving wall. Therefore, the drop stabilizes at an equilibrium position in the upper half plane at small to moderate Capillary numbers (0.0048 to 0.12).

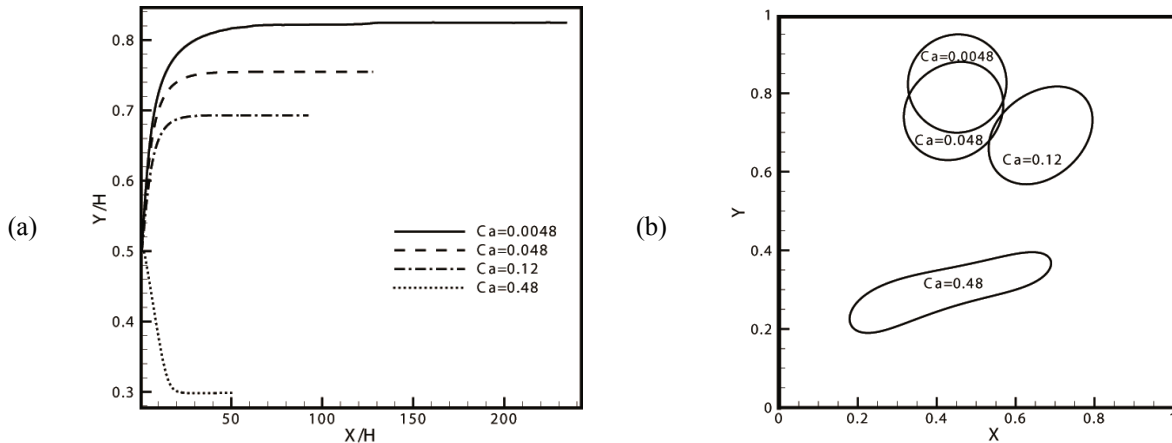


Fig. 6. Effect of deformation on the lateral equilibrium position, $Re_b = 40$, $Fr = 10$ and $\rho_i/\rho_o = 1.05$, (a) lateral position versus axial location, (b) drop shape at different Capillary numbers.

The equilibrium position moves towards the center of the channel with increasing Capillary number due to the enhancement of the wall repulsion force. However, the magnitude of the slip velocity also increases as the Capillary is raised (not plotted). At the largest Capillary number (0.48) the drop migrates to an equilibrium position in the lower half plane due to the large negative slip velocity. We note that the drop elongates to a large extent at this Capillary number, which shows the onset of break up.

Similar results have been derived at a density ratio less than one (Fig. 7a). Here, since the slip velocity is positive, the rotational lift is towards the stationary wall. The drop migrates to an equilibrium position in the lower half plane at a small Capillary number (0.0048). The drop gets a prolate shape like a rising bubble (Fig. 7b). At a large Capillary number (0.048), the drop moves to the upper half plane due to a large positive slip velocity. In other words, the drift due to the stationary wall forces the drop to the upper half plane. This is similar to the case observed with a density ratio greater than one.

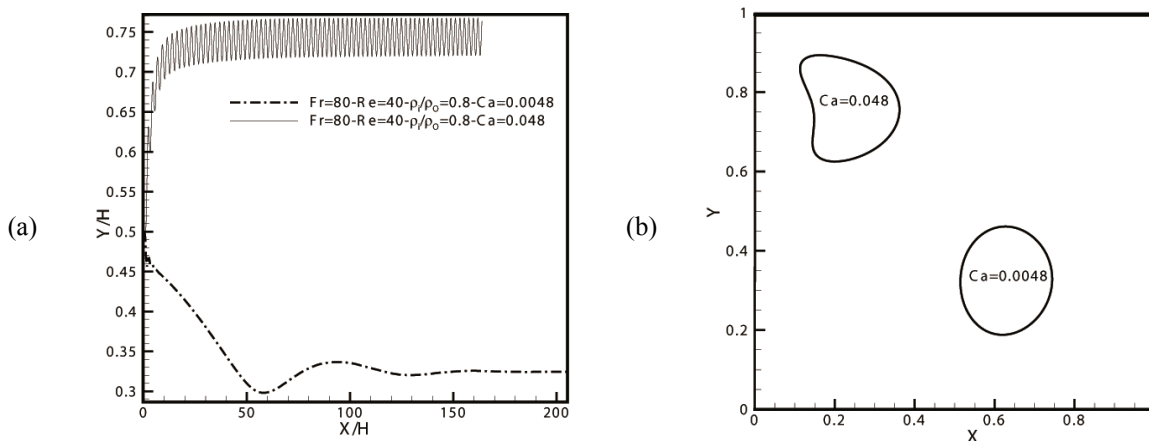


Fig. 7. Effect of deformation on the lateral equilibrium position, $Re_b = 40$, $Fr = 80$ and $\rho_i/\rho_o = 0.8$, (a) lateral position versus the axial location, (b) drop shape at two Capillary numbers

There are some oscillations with small amplitude in the equilibrium position at this Capillary number. This is due to an unstable drop shape at this relatively large Capillary number. The drop shape changes as it moves along the channel. This is shown in Fig. 8.

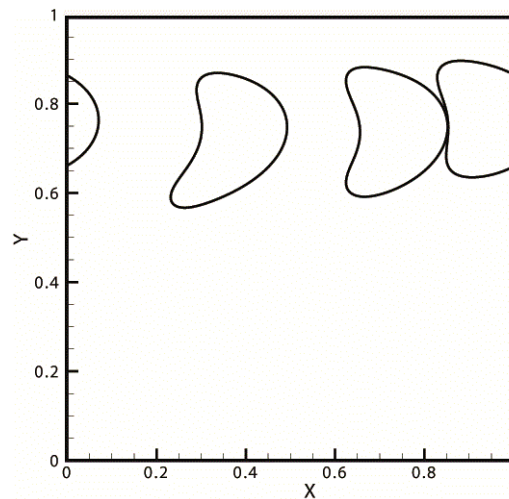


Fig. 8. Unstable drop shape for $Re_b = 40$, $Fr = 80$, $\rho_i/\rho_o = 0.8$ and $Ca = 0.048$

The equilibrium position is plotted against the Capillary number in Fig. 9 for two density ratios. At a density ratio greater than one, the equilibrium position moves towards the stationary wall with increasing the Capillary number. When the density ratio is less than one, the equilibrium position moves towards the moving wall.

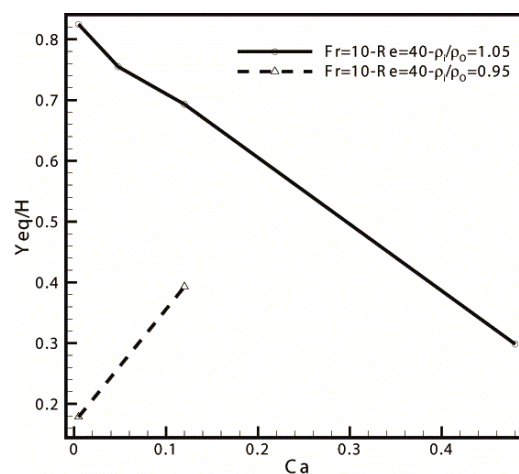


Fig. 9. Equilibrium position of drop versus Capillary number for two density ratios, $Re_b = 40$ and $Fr = 10$

d) Effect of the Froude number

The effect of the Froude number on the lateral equilibrium position was studied by considering several density ratios and two Reynolds numbers. Figure 10 presents the equilibrium position versus the Froude number for different density ratios. At density ratios close to one (0.998, 1.002), the equilibrium position moves towards one of the walls as the Froude number is raised. This is mainly due to the rotational lift that is enhanced with increasing the Froude number. For slightly buoyant drops ($\rho_i/\rho_o = 0.95, 1.002$), the rotational lift is the dominant mechanism that determines the lateral equilibrium position of the drop. For a density ratio of 1.002, two Reynolds numbers were considered ($Re_b = 10, 40$). It is observed that the equilibrium position moves to the moving wall at the larger Reynolds number. (The effect of Reynolds number will be addressed in the next section).

At a lower density ratio (0.95), the equilibrium position first moves towards the stationary wall, but it goes back to the midplane at higher Froude number. At large Froude numbers, the slip velocity becomes large, so the drift by the wall (lubrication effect) increases. This moves the equilibrium position back to the midplane. The phenomenon is similar to that observed at large or low density ratios in section 4.2. At the largest Froude number (392) the drop obtains a prolate shape due to large slip velocity. This results is new in this flow type. The streamlines for this drop are also plotted in Fig. 11, which resembles a rising bubble.

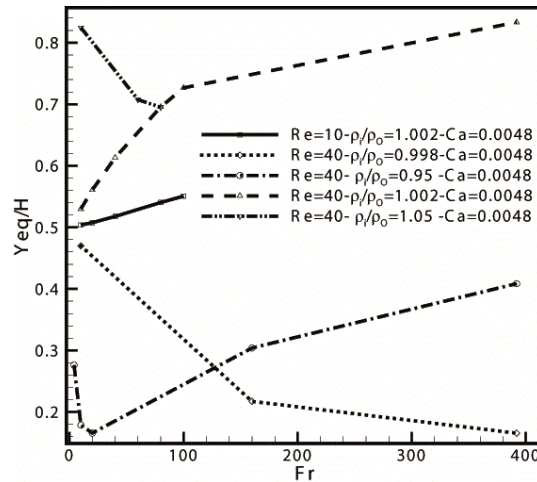


Fig. 10. Equilibrium position of drop versus Froude number for several density ratios

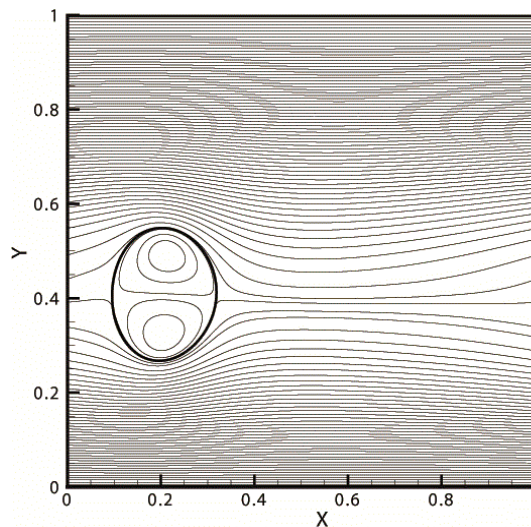


Figure 11. Streamlines for a drop at stable equilibrium position, $Re_b = 40$, $Fr = 392$, $Ca = 0.0048$ and $\rho_i/\rho_o = 0.95$

At a relatively large density ratio (1.05), the equilibrium position lies in the upper half plane, and moves towards the midplane with increasing the Froude number (Fig. 10). As the Froude number increases, the slip velocity gets even larger, so the wall repulsion force enhances. This moves the drop to an equilibrium position closer to the midplane. We note that if the Froude number gets even larger (> 80), the drop may not obtain a stable equilibrium position. (This has been examined for $Fr = 392$ at $\rho_i/\rho_o = 1.05$).

The migration velocity of the drop is plotted versus time for different Froude numbers in Fig. 12. The migration velocity increases as the Froude number is raised. As a result, the drop reaches the steady state equilibrium position in a shorter period.

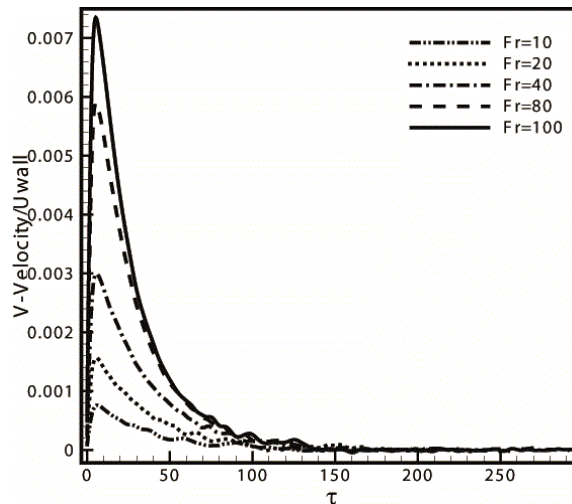


Fig. 12. Migration velocity of drop versus time for different Froude numbers, $Re_b = 40$, $Ca = 0.0048$ and $\rho_i/\rho_o = 1.002$.

e) Effect of the Reynolds number

Results showing the effect of Reynolds number on the equilibrium position of a drop for a range of density ratios and Froude numbers are presented in this section. The equilibrium position is plotted versus the Reynolds number in Fig. 13. For density ratios close to one (0.998 or 1.002), the equilibrium position moves either towards the stationary wall ($\rho_i/\rho_o = 0.998$), or towards the moving wall ($\rho_i/\rho_o = 1.002$), as the Reynolds number is raised. In other words, for slightly buoyant drops, the equilibrium position moves towards the walls as the Reynolds number is increased. This is due to enhancement of the inertial lift and also an increase in the slip velocity. The slip velocity (not plotted here) increases in magnitude with the Reynolds number. For a density ratio of 1.002, two Froude numbers (40,392), which show similar trends were examined. However, at a lower density ratio (0.95), the equilibrium position moves back to the midplane with increasing the Reynolds number. We emphasize that the Froude number is the same for the two density ratios less than unity. As a result, for more buoyant drops the equilibrium position moves away from the wall with increasing the Reynolds number. The behavior can be addressed by large slip velocity for low density ratio (0.95). Here, the large slip velocity increases the wall repulsion force, which in turn moves the equilibrium position towards the midplane.

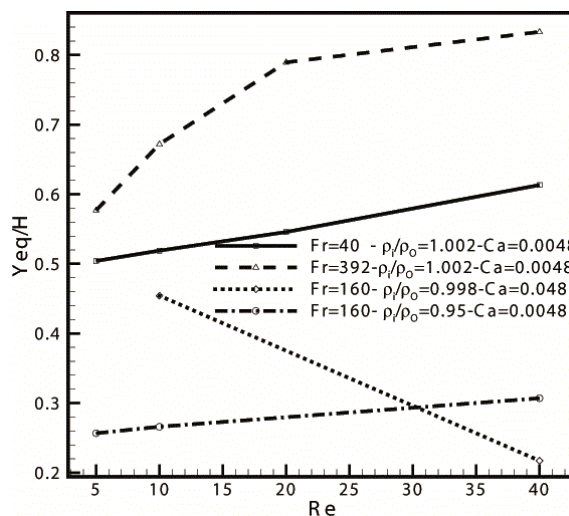


Fig. 13. Equilibrium position versus Reynolds number for different Froude numbers and density ratios

We note that the drop may not obtain a stable equilibrium position at large Reynolds numbers. This is illustrated in Fig. 14a, where a larger Reynolds number has been examined ($Re_b = 80$). The drop oscillates in the lower half plane with a finite amplitude. The simulation was checked by considering a higher grid resolution (384×384). The amplitude of oscillations does not change as far as the simulation has proceeded. The type of oscillations observed here has also been seen by Mortazavi and Tryggvason [11] at large Reynolds numbers in Poiseuille flow. The drop shapes are also plotted in Fig. 14b for two Reynolds numbers. Due to higher slip velocity at higher Reynolds number, the drop gets a prolate shape at larger Reynolds number. This shows that the effect of the external shear field on drop deformation is not significant at large slip velocities.

It should be pointed out that the results obtained here are new in the sense that they are obtained for deformable drops at finite Reynolds numbers. There are no results available to make a quantitative comparison. Results that are only for solid particles and qualitative comparison were made as above.

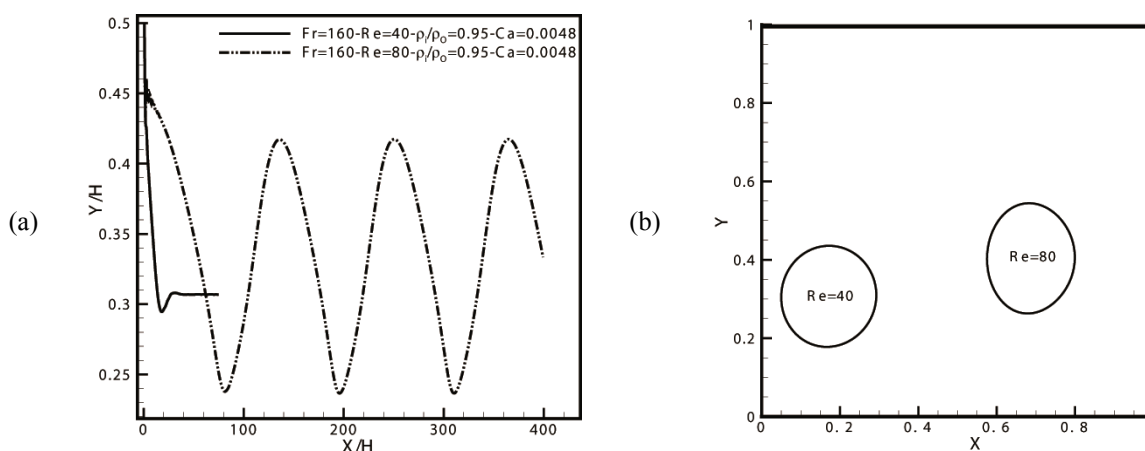


Fig. 14. (a) Lateral position versus the axial location for two Reynolds numbers, $Re_b = 40, 80$, (b) drop shapes for these Reynolds numbers

5. CONCLUSION

A two-dimensional study of the motion of a drop suspended in a simple shear flow under the action of gravity force was performed numerically. Based on the results obtained, the following conclusions can be drawn:

1. At density ratios less than unity, but close to one, the equilibrium position moves towards the stationary wall. When the density ratio is low enough, equilibrium position moves back to the midplane. This is due to enhancement of the wall repulsion force. At density ratios larger than one but close to unity, the equilibrium position moves towards the moving wall. As the density ratio is raised, the equilibrium position moves back to the midplane. Results are in agreement with numerical simulations performed by Feng et al. [8], and the perturbation theory of Vassur and Cox [4]. However, the behavior observed at small or large density ratios does not agree with the perturbation theory.
2. Drops which are sufficiently deformable move closer to the midplane. For a lagging drop, the equilibrium position moves to the midplane as the Capillary number is increased. At large Capillary numbers, the drop moves towards the stationary wall. The drop may not obtain a stable equilibrium shape at large Capillary numbers. As a result, the equilibrium position shows small oscillations around a position close to the moving wall (for a leading drop). This is a new phenomenon observed in this limit.
3. For slightly buoyant drops, the equilibrium position moves to the walls as the Froude number is raised. For a moderately buoyant drop, the equilibrium position moves towards the midplane with increasing the Froude number.

4. For slightly buoyant drops, the equilibrium position moves to the walls with increasing the Reynolds number. This is mainly due to enhancement of the slip velocity of the drop, which in turn increases the rotational lift. However, at a relatively large buoyancy force, the equilibrium position moves slightly towards the midplane. This is due to an increase of the wall repulsion force. At a relatively large Reynolds number (80) and a moderate Froude number (160), the drop does not obtain a stable equilibrium position. Instead, the drop oscillates with a finite amplitude around an equilibrium position in the lower half plane (when the drop leads the flow). This is also a new behavior that is observed in the current work.

Finally, behavior observed here for the motion of a single drop may be generalized to many drop interactions at some flow conditions. Preliminary results show that suspension of drops at low area fraction follow the motion of a single drop in a channel. This subject is left for future investigations.

REFERENCES

1. Taylor, G. I. (1934). The deformation of emulsions in definable fields of flow. *Proc R Soc (London)*, A146, pp 501–523.
2. Karnis, A. & Mason, S. G. (1967). Particle motions in sheared suspension, Part 23: Wall migration of fluid drops. *J. Colloid Interface Sci.*, Vol. 24, pp. 164-69.
3. Halow, J. S. & Wills, G. B. (1970). Radial migration of spherical particles in Couette systems. *AICHE J.*, Vol. 16, pp. 281-286.
4. Vasseur, P. & Cox, R. G. (1976). The lateral migration of a spherical particle in two-dimensional shear flows. *J. Fluid Mech.*, Vol. 78, pp. 385-413.
5. Ho, B. P. & Leal, L. G. (1974). Inertial migration of rigid spheres in two-dimensional unidirectional flows. *J. Fluid Mech.*, Vol. 65, pp. 365-383.
6. Zhou, H. & Pozrikidis, C. (1993). The flow of suspensions in channels: single files of drops. *Phys Fluids*, Vol. A5, No. 2, pp. 311–324.
7. Zhou, H. & Pozrikidis, C. (1993b). The flow of ordered and random suspensions of two-dimensional drops in a channel. *J. Fluid Mech.*, Vol. 255, pp. 103-127.
8. Feng, J., Hu, H. H. & Joseph, D. D. (1994). Direct simulation of initial value problems for the motion of solid bodies in a Newtonian fluid. Part 2. Couette and Poiseuille flows. *J Fluid Mech.*, Vol. 277, pp. 271–301.
9. Saffman, P. G. (1965). The lift on a small sphere in a slow shear flow. *J. Fluid Mech.*, Vol. 22, pp. 385-400.
10. Kapil, S. S. & Pozrikidis, C. (1995). Effects of inertia on the deformation of liquid drops in simple shear flow. *Computers and Fluids*, Vol. 24, pp. 101-119.
11. Mortazavi, S. & Tryggvasson, G. (1999). A numerical study of the motion of drop in poiseuille flow, Part 1: lateral migration of one drop. *J. Fluid Mech.*, Vol. 411, pp. 325–350.
12. Matas, J. P., Morris, J. F. & Guazzelli, E. (2004). Lateral forces on a sphere. *Oil and gas science and technology. Rev. IFP*, Vol. 59, pp 59-70.
13. Liu, T. & Lu, X. (2004). Numerical simulation of drop migration in channel flow under zero-gravity. *Acta Mechanica Sinica*, Vol. 20, pp. 199–205.
14. Lin, C. & Guo, L. (2007). Experimental study of drop deformation and breakup in simple shear flows. *Chin. J. Chem. Eng.*, Vol. 15, pp. 1-5.
15. Bayareh, M. & Mortazavi, S. (2009). Numerical simulation of the motion of a single drop in a shear flow at finite Reynolds numbers. *Iranian Journal of Science & Technology Transaction B: Engineering*, Vol. 33, pp. 441–452.
16. Mortazavi, S., Afshar, Y. & Abbaspour, H. (2011). Numerical simulation of two-dimensional drops suspended in simple shear flow at nonzero Reynolds numbers. *Journal of Fluids Eng.*, Vol. 133, pp. 1-9.

17. Unverdi, S. O. & Tryggvason, G. (1992a). A front tracking method for viscous incompressible flows. *J. Comput. Phys*, D100, pp. 25-37.
18. Unverdi, S. O. & Tryggvason, G. (1992b). Computations of multi-fluid flows. *Physica*, D60, pp. 70-83.
19. Adams, J. (1989). MUDPACK: Multigrid FORTRAN software for the efficient solution of linear elliptic partial differential equations. *Appl. Math. Computer*, Vol. 34, pp. 113-144.
20. McLaughlin, J. B. (1991). Inertial migration of a small sphere in linear shear flow. *J. Fluid Mech.*, Vol. 224, pp. 261-274.